Computers and Concrete, *Vol. 23, No. 2 (2019) 121-131*
DOI: https://doi.org/10.12989/cac.2019.23.2.121

Improved nonlinear modelling approach of simply supported PC slab under free blast load using RHT model

Mohamed Rashad[1a] and T.Y. Yang[*1,2]

[1]*Department of Civil Engineering, University of British Columbia, Vancouver, Canada*
[2]*International Joint Research Laboratory of Earthquake Engineering, Tongji University, Shanghai, China*

(Received April 21, 2018, Revised January 31, 2019, Accepted February 6, 2019)

Abstract. Due to the heterogeneity nature of the concrete, it is difficult to simulate the hyperdynamic behaviour and crack trajectory of concrete material when subjected to explosion loads. In this paper, a 3D nonlinear numerical study was conducted to simulate the hyperdynamic behaviour of concrete under various loading conditions using Riedel-Hiermaier-Thoma (RHT) model. Detailed calibration was conducted to identify the optimal parameters for the RHT model on the material level. For the component level, the calibrated RHT parameters were used to simulate the failure behaviour of plain concrete (PC) slab under free air blast load. The response was compared with an available experimental result. The results show the proposed numerical model can accurately simulate the crack trajectory and the failure mode of the PC slab under free air blast load.

Keywords: 3D nonlinear finite element analysis; RHT model; plain concrete; free air blast load; mesh sensitivity

1. Introduction

The nonlinear behaviour of concrete structures can be modelled using mesoscale and macro-scale approaches (Hentz *et al*. 2004, Govindjee *et al*. 1995, Malvar *et al*. 1997, Gebbeken and Ruppert 2000). The mesoscale modelling is more advanced but more complicated and time-consuming. Usually, the macro model is computationally more efficient, but not able to accurately predict the localized damage of concrete structure. In this study, a robust 3D macro model, based on the Riedel-Hiermaier-Thoma (RHT) model (Riedel *et al*. 1999, Riedel 2000, Riedel *et al*. 2008, Riedel 2009), was used to simulate the nonlinear dynamic response of concrete structures under blast load. Detailed geometric and material nonlinearities were considered in the numerical model.

In the past, a serious of modified RHT models have been used to simulate the nonlinear response of different concrete structures (Tu and Lu 2009, Tu and Lu 2010, Hu *et al*. 2016, Nystrom and Gylltoft 2009, Nystrom and Gylltoft 2011, Wang *et al*. 2013, Codina *et al*. 2016). The simulation results of these studies show that the proposed RHT models can predict the dynamic behaviour of concrete against blast loads. Tu and Lu (2009, 2010) examined and evaluated the concrete nonlinear dynamic behaviour using the RHT model with the default parameters implemented in Autodyn (ANSYS-AUTODYN 2009) (referred from hereon as the default RHT model). It was found that the default RHT model gives unsatisfactory behaviour under blast loads. Accordingly, they modified the default parameters to improve the accuracy of the numerical model to simulate the nonlinear behaviour of a one-way reinforced concrete (RC) slab fixed from the two short sides and subjected to confined blast load. The result shows that the proposed modified parameters can simulate the crack patterns observed in the physical test better than the default parameters. Similarly, Hu *et al*. (2016) proposed another modified RHT model to better simulate the blast behaviour of a plain concrete (PC) slab fixed to the ground using four anchors at four corners. The PC slab was subjected to a close-in blast load at a standoff distance (SoD) of 170 mm above the specimen. It was found that the default RHT model underestimates the crack pattern and crater diameter. In contrast, the proposed RHT model decreases the ductility of the model to better estimate the crack pattern and crater diameter observed during experimental test. Wang *et al*. (2013) used the modified RHT model proposed by Tu and Lu (2009, 2010) with a slight change in the reference density and failure strain to simulate the blast behaviour of a one-way RC slab subjected to close-in blast load. By comparing the numerical results with the experimental results, it was found that the modified RHT model can model the crack patterns well but slightly overestimates the concrete spalling. Similarly, Codina *et al*. (2016) modified some of the RHT parameters and used them to simulate the behaviour of RC column against blast loads at short distance. In addition, they compared their proposed parameter with the modified RHT parameters proposed by Tu and Lu (2009, 2010). It was found that the default and the proposed RHT parameters by Tu and Lu show more significant damage contours than that observed on the physical tests. In contrast, the modified parameters developed by Codina *et al*. (2016) can provide a more accurate prediction of the damage pattern and maximum displacement. Similarly, Nystrom and Gylltoft (2009)

∗Corresponding author, Professor
E-mail: yang@civil.ubc.ca
[a]Ph.D. Candidate
E-mail: mohamed.rashad@alumni.ubc.ca

http://www.techno-press.org/?journal=cac&subpage=8 ISSN: 1598-8198 (Print), 1598-818X (Online)

proposed another set of modified RHT parameters to simulate the blast behaviour of a simply supported RC wall subjected to blast loads.

In general, all the aforementioned modified RHT parameters can be used to model the hyperdynamic response of concrete structure. However, the accuracy of the model varied significantly with the specimen dimensions, loading conditions, boundary and initial conditions. Based on the numerical investigation presented in this paper, the aforementioned RHT parameters cannot accurately model the nonlinear behaviour of simply supported PC slab under free blast load. Hence, in this study, a new set of RHT parameters were proposed to accurately simulate the damage pattern and the crack trajectory of simply supported PC slab subjected to free air blast load.

The newly proposed RHT parameters were used to simulate the nonlinear behaviour of the concrete material under unconfined uniaxial, equal biaxial and triaxial tension and compression tests. The stress-strain curves show that the newly proposed RHT model can more accurately simulate the strain softening behaviour of concrete material than the default RHT model.

In addition to the material level comparison, an experimental test of a simply supported PC slab under free blast load was conducted. The crack trajectory and damage pattern observed from the experimental test and the nonlinear numerical simulation were compared. The result shows that by using the newly proposed parameters, the RHT model can accurately simulate the blast behaviour of PC slab under free air blast loads.

2. Theory of RHT model

RHT material model employs three strength surfaces to define the elastic limit surface (or initial surface), failure surface and residual surface (or post-failure surface) as shown in Fig. 1.

The three surfaces can be expressed using the following equations:

$$Y_{\text{elastic}} = Y_{\text{failure}} \text{ x } F_{\text{elastic}} \text{ x } F_{\text{cap}} \tag{1}$$

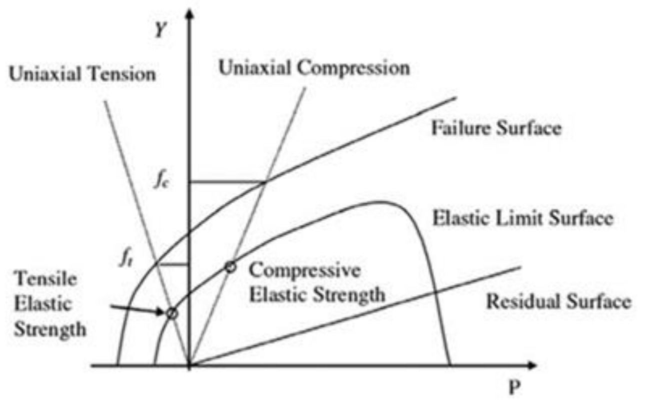

Fig. 1 Three strength surfaces of RHT model (Riedel *et al*. 1999)

$$Y_{\text{failure}} = Y_{\text{TXC}}\,(p) \text{ x } R_3(\theta) \text{ x } F_{\text{rate}}(\dot{\varepsilon}) \tag{2}$$

$$Y_{\text{residual}} = f_{\text{C}} \text{ x } B \text{ x } \left(\frac{p}{f_{\text{C}}}\right)^M \tag{3}$$

Where Y_{elastic} is the elastic limit surface; Y_{failure} is the failure surface; F_{elastic} the ratio of the elastic strength to failure strength along a radial path; F_{cap} is a parabolic function; $Y_{\text{TXC}}\,(p)$ is the compressive meridian which is a function of hydrostatic pressure (p); $R_3(\theta)$ is a reduction factor of the failure surface Y_{failure}, which is a function of the Lode angle (θ), which represent the rotation about the hydrostatic axis; $F_{\text{rate}}(\dot{\varepsilon})$ is the dynamic amplification factor (DIF) as a function of strain rate $\dot{\varepsilon}$; Y_{residual} is the residual surface; f_{C} is the uniaxial compressive strength; B is the fractured strength constant and M is the fractured strength exponent.

In this study, a modification has been applied to the some effective RHT strength and failure model parameters (B, M, D_1, D_2 and e_{min}^{fail}). These nominated parameters are which are. B and M, as illustrated in Eq. (3), control the residual and affect the post-failure surfaces. While D_1, D_2 and e_{min}^{fail}, as illustrated in Eqs. (4), (5) and (6), control the concrete post-softening behaviour.

$$D = \int_0^{\varepsilon_p} \left(\frac{\Delta\varepsilon_p}{D_1 \left(p^* - {f_t}/{f_c}\right)^{D_2}} \right) \quad for\ D_1 \left(p^* - {f_t}/{f_c}\right)^{D_2} > e_{min}^{fail} \tag{4}$$

$$D = \int_0^{\varepsilon_p} \left(\frac{\Delta\varepsilon_p}{e_{min}^{fail}} \right) \quad for\ D_1 \left(p^* - {f_t}/{f_c}\right)^{D_2} < e_{min}^{fail} \tag{5}$$

$$e_{min}^{fail} = \frac{2\ x\ G_f}{\sigma_t\ x\ L_{eq}} \tag{6}$$

Where D is the damage parameter; $\Delta\varepsilon_p$ is the plastic strain increment; D_1 and D_2 are the shape parameters; $p^* = p/f_c$ is the normalized pressure variable; G_f is the fracture energy; σ_t is the tensile failure stress; L_{eq} is the characteristic length of the element (the diameter of a sphere having the same volume of the 3D element (ANSYS- AUTODYN 2009)).

These modified parameters were defined to ensure a more realistic strain softening range, for both tension and compression loading conditions. Table 1 shows the main effective parameters of the default and the newly proposed RHT models in this study.

Table 1 Main parameters of the default and proposed RHT model

Parameters	Default RHT model	Proposed RHT model
Fractured Strength Constant B	1.6	0.9
Fractured Strength Exponent M	0.61	0.9
Damage Constant D_1	0.04	0.02
Minimum Strain to Failure e_{min}^{fail}	0.01	0.002

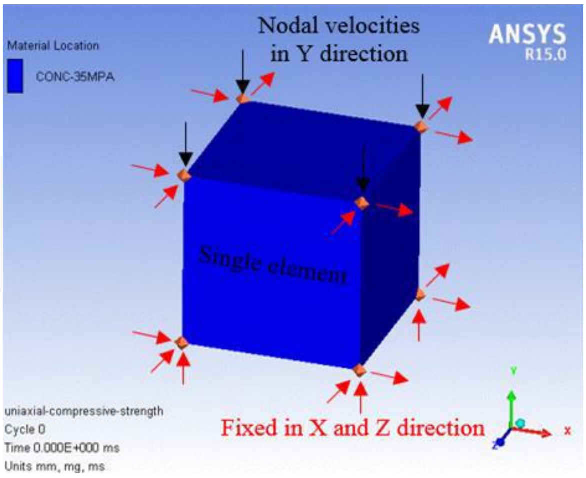

Fig. 2 Uniaxial numerical compression test

3. Numerical analyses on a single concrete finite element

To simulate the influence of the newly proposed RHT parameters on the material level, a single concrete element with size 10 mm subjected to unconfined uniaxial compression and tension loading condition, equal biaxial compression and tension loading condition, triaxial tension loading condition and triaxial compression loading condition with different levels of confinement (1 MPa, 5 MPa, 10 MPa and 20 MPa) were simulated. The single concrete element is modelled as a Lagrangian element (ANSYS-AUTODYN 2009). The loads are applied by moving the four nodes perpendicular to the element surface with a constant velocity. To avoid the influence of the strain rate effect, a suitable velocity should be applied to the single element. After applying some trials on the unconfined uniaxial test, a nodal velocity of value 10-5 m/s was chosen which can achieve the desired yield strength value. It should be noted that a smaller nodal velocity can be used, but it will significantly increase the computational time. The boundary conditions were constrained such that the element can only deform under the direction of the load without any shear stresses. Fig. 2 shows the finite element model developed for this study.

Figs. 3 and 4 show the comparison between the axial stress-strain curves of the concrete material using the default RHT model and the newly proposed RHT model under different loading cases. The results show that the default RHT model overestimate the strain softening range for both the tension and compression tests based on the common experimental results (Chen 1982, Malvar *et al*. 1997, Zhang *et al*. 2007, Tu and Lu 2009). It was found that the proposed RHT parameters improve the post-yield softening behaviour of the stress-strain curves under the different compression and tension loading patterns. Under the tensile case, the softening behaviour was enhanced and the minimum failure strain e_{min}^{fail} was decreased to a reasonable value which showed a more accurate failure pattern when compared with the corresponding experimental results (Chen 1982, Malvar *et al*. 1997). For compression tests, the default RHT model shows unrealistic

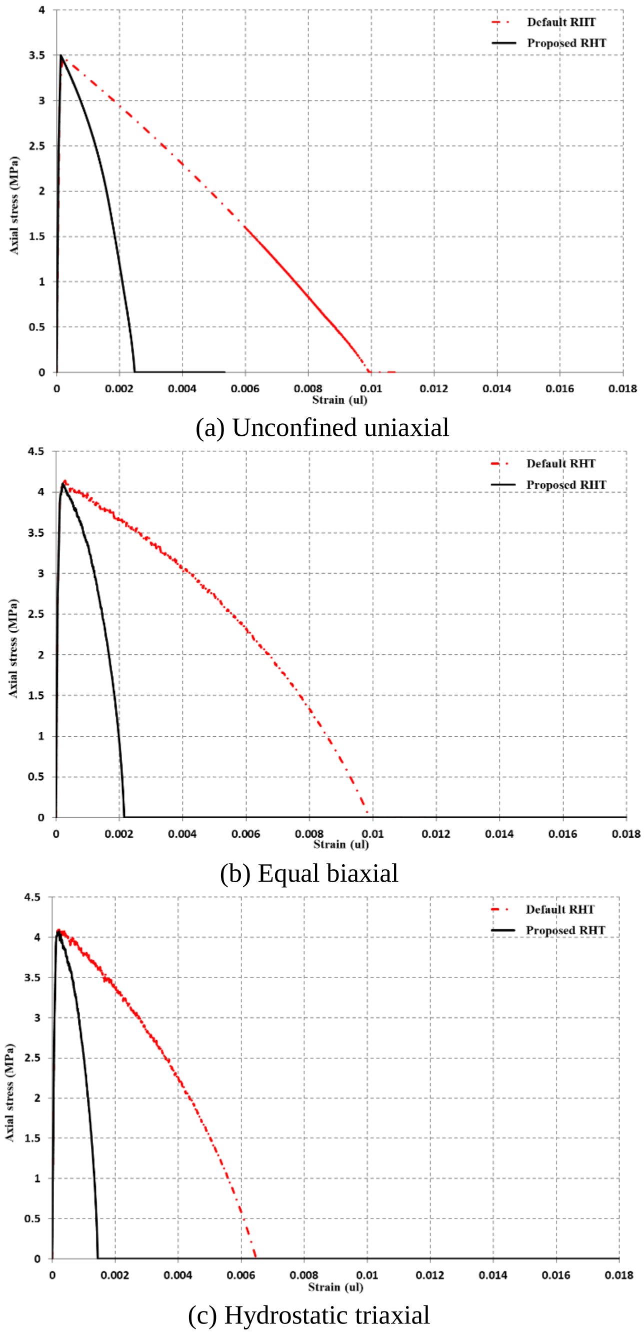

Fig. 3 Axial stress-strain curves of the default and proposed RHT model for tension

high residual strength after reaching the failure strength, as shown in Fig. 4. This is attributed to the simplification of the residual strength surface in the default RHT model which exhibits a circular deviatoric cross section plane in the principle stress space. This inaccurate softening behavior was strongly modified by changing the value of the Fractured Strength constant (B) and Fractured Strength Exponent (M) which control the final residual strength. Accordingly, a considerable reduction occurred on the final residual strength and the compression failure strain, as shown in Fig. 4, which became more acceptable compared with the corresponding laboratory tests (Zhang *et al*. 2007). In addition, the damage Constant (D1) was decreased to

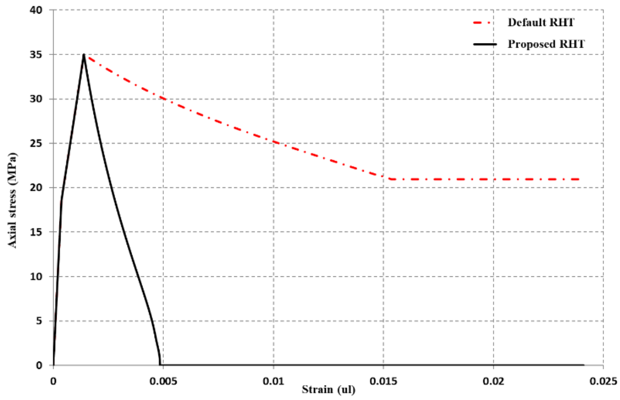

(a) Unconfined uniaxial

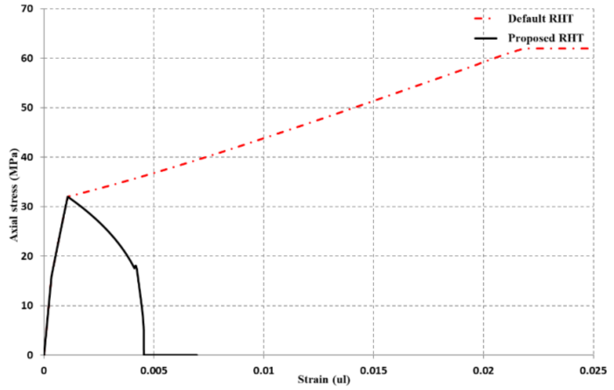

(b) Equal biaxial

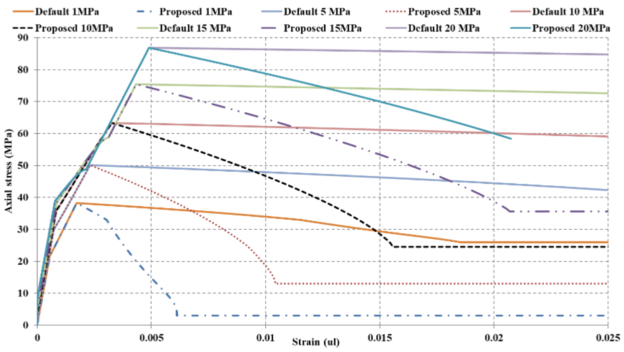

(c) Triaxial with levels of confinement

Fig. 4 Axial stress-strain curves of the default and proposed RHT model for compression

better simulate the degrading portion of the concrete material. For the triaxial compression test, it can be noted that with the increasing of the confining level, the maximum compression strength increases which is agreed with the general experimental results. In addition, based on similar experimental results (Malvar *et al*. 1997, Lu and Hsu 2007), an enhancement occurred in the post softening curve and the residual strength for each confinement level compared with that obtained by using the default RHT model.

4. Experimental and numerical application on a PC slab against free air blast load

4.1 Experimental test

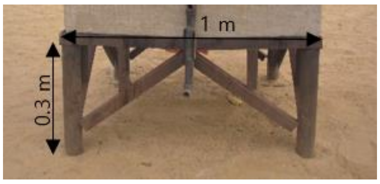

(a) Test rig

(b) Explosion process

(c) PC slab after applying the blast load

Fig. 5 Test rig and the PC slab used in the experimental test

In order to examine and evaluate the capability of the proposed RHT model parameters, an experimental test on a simply supported PC slab subjected to free air blast load, as shown in Fig. 5(b and c), was conducted. The dimension of the specimen was square 1 m x 1 m and thickness of 20 cm. In this test, the PC slab was subjected to 4 Kg TNT detonated at SoD of 1 m. A field test rig, as shown in Fig. 5(a), was used to simulate the simply supported boundary conditions of the PC slab at four edges.

To properly record the actual pressure experienced by the specimen, a simple free air blast test, using 1 Kg TNT at SOD of 1m, was conducted and the pressure time history was recorded by a pressure sensor, as shown in Fig. 6(a). The recorded Pressure time history was then compared with that calculated by the CONWEP program (CONWEP 1990), as shown in Fig. 6(b). The results show an excellent agreement between the two pressure time histories.

After this verification, the PC slab was tested under 4 Kg TNT at SoD of 1 m. A high-speed camera, which can depict real photos and create graphical movies at 20000 frames/sec, was used. The spreading of the fireball, the front shock wave (compressed air layer) and its reflection with the specimen surface and the ground were observed, as shown in Fig. 5(b). A comparison between the experimental, analytical and numerical pressure time histories will be illustrated later.

4.2 Numerical analysis

To simulate the nonlinear behavior of the PC slab against blast load, a numerical model, as shown in Fig. 7, was developed. Due to the double axis of symmetries, only a quarter numerical model was developed. More than 2.3 million elements are used for the numerical model. Consistent boundary conditions were applied to simulate a similar environment as in the arena test. Flow out boundary condition was applied to the outer faces of the air block except for the symmetric faces. In this study, a fluid-

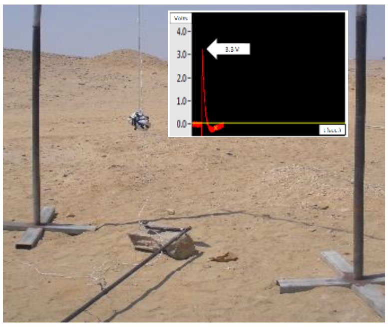

(a) Field test (Pressure sensor)

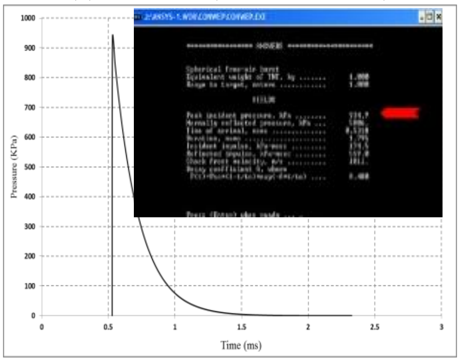

(b) Pressure time history (CONWEP)

Fig. 6 Free air explosion test of 1Kg TNT

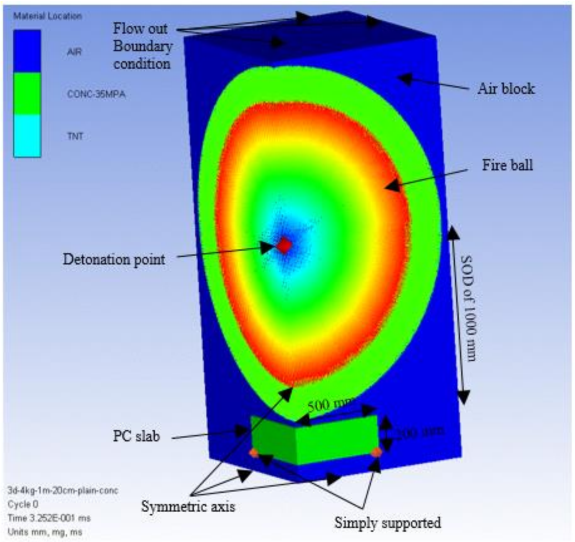

Fig. 7 A quarter numerical model of the PC panel

structure coupling algorithm was used to apply the blast load on the PC slab. The methodology of this algorithm is that air and explosion environment are modelled by Eulerian process, which can represent large deformation through fixed meshes. These Eulerian meshes exert a pressure boundary condition on the Lagrangian meshes, which represent the PC slab. Accordingly, Lagrangian elements experience deformation through the fixed Eulerian meshes and also exert a velocity boundary condition to the Eulerian material flow. Finally, the response of the PC slab against explosion load can be analyzed in a single numerical model using the coupled Lagrangian-Eulerian algorithm (Benson 1992).

Table 2 Material data of air and TNT used in the model

Material	Air	TNT	TNT (Ideal)
Equation of State	Ideal Gas	JWL	Ideal Gas
Initial Conduction	ρ=1.225×10^{-3} g/cm^3	Default	From Detonation
Density	1.225×10^{-3} g/cm^3	Library Data	1.0×10^{-3} g/cm^3
Ideal Gas Constant	γ=1.4	Standard	γ=1.35
Reference Energy	2.068×10^5 μJ/mg		Model/remap data

Table 3 Summary of the parameters used to model TNT

JWL Parameter	TNT
A (GPa)	373.75
B (GPa)	3.747
*R*1	4.15
*R*2	0.90
w	0.35

4.2.1 Numerical modelling of the explosion

To properly model the hyperdynamic behaviour of the TNT explosion, a numerical analysis was performed to simulate the aforementioned free air blast test in which a 1 Kg TNT detonated at SoD of 1 m. The numerical result was compared with that measured in the field and that calculated by empirical equations provided by TM5 (TM5-1300 1990), implemented in CONWEP. In this model, the air was modelled using the Hydro (ideal gas) equation of state (EOS) which can be written in the form of Eq. (7) (ANSYS 2007). TNT was modelled using the Jone Wilkins-Lee (JWL) model (ANSYS 2007) which can be written in the form of Eq. (8). More details about Air and TNT modelling can be found in our previous work (Rashad and Yang 2018 and 2019). Table 2 shows the property of the air and TNT used in this study.

$$P_{EOS} = (\gamma - 1)\rho e \tag{7}$$

Where P_{EOS} is the pressure; γ is a constant; ρ is air density; e is the specific internal energy.

$$P_{EOS} = A\left(1 - \frac{w}{R_1 V}\right)e^{-R_1 V} + B\left(1 - \frac{w}{R_2 V}\right)e^{-R_2 V} + w\frac{E}{V} \tag{8}$$

where P_{EOS} is the hydrostatic pressure; *A*, *B*, R_1, R_2 and *w* are the JWL parameters that are used to model the air and TNT material; *V* is the ratio of ρ_{SOL}/ρ, where ρ is the current density and ρ_{SOL} is the density of solid explosive; $E = \rho_{SOL}\, e_{int}$ is the internal energy per unit volume of the explosive, where e_{int} is the current internal energy per unit mass; The specific values are outline in Table 3. The first and second terms of the right-hand side of the JWL equation of state become negligible at expansions of approximately ten times the original volume. Therefore, at these large expansions, it is common practice to simplify the equation of state used to that of an ideal gas.

After creating 2D model, the pressure is mapped into a 3D coupled finite element model. In the 3D model, Euler-FCT (Flux corrected Transport) formulation was used to solve the nonlinear dynamic response of the air. The boundary condition of the surrounding air is chosen as flow

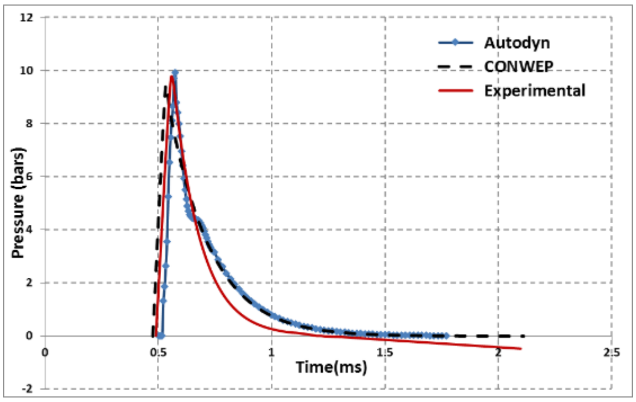

Fig. 8 Comparison of the Pressure time histories of 1 kg TNT at SOF of 1 m (Rashad and Yang 2019)

Table 4 Comparison between the peak overpressure values

Empirical Equations	Field blast test	Numerical Simulation
9.35 bar	9.65 bar	9.91 bar

out at all the faces of the air block except the symmetric ones.

Fig. 8 shows the comparison of the pressure time history of 1 Kg TNT detonated at SoD of 1 m between the numerical simulation, the empirical result obtained from the CONWEP program and the experimental results. Table 4 shows the peak overpressure values calculated by using the empirical equations, measured from the experiment and that simulated by using AUTODYN. It was found that the proposed modelling technique approach is very effective to simulate blast loading. The trend of the pressure-time history calculated by the 3D Coupled FEA is almost the same as that obtained from the field test. The numerical result overestimated the measured peak overpressure value by 2.6% and the empirical equations, implemented in CONWEP, underestimated it by 3.1%. The results show that the numerical pressure time history is more reliable than that calculated by the CONWEP program. In addition, the numerical modelling of the explosion process can simulate the realistic distribution of the blast load on the specimen and the wrap over effect of the fire ball which occurs on the physical tests.

4.2.2 Numerical modelling of the PC slab

In this study, concrete was modelled using both the porosity EOS and the polynomial solid EOS which can be written in the form of Eqs. (9) and (10), respectively. This EOS is capable of simulating the thermodynamic and the compaction behaviour of concrete at different levels of pressure (Herrmann 1969). Fig. 9 shows the $p{-}\propto$ relationship which represents the porosity EOS and $p-\rho$ relationship which represents the solid EOS, respectively.

$$\propto = 1 + (\propto_p - 1)\left[\frac{p_s - p}{p_s - p_e}\right]^n , \propto = \frac{v}{v_s} \tag{9}$$

Where $\propto_p$ is porosity corresponding to the initial plastic yield; p is current pressure, n is the compaction exponent; v is the specific volume of the porous material and v_s is the specific volume of the concrete in the solid state at the same pressure and temperature. v_s is equal to $1/\rho_s$ at zero pressure, and ρ_s is solid density, that is the density at zero pressure of a fully compacted solid.

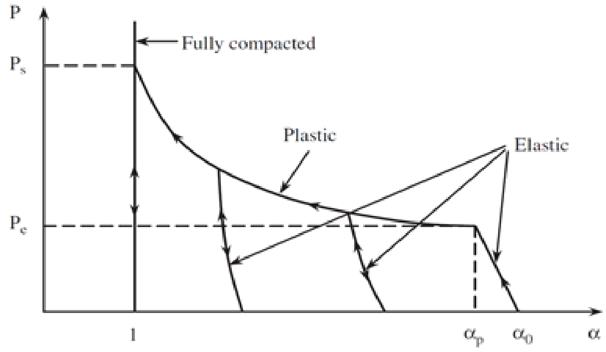

(a) p-$\propto$ relationship

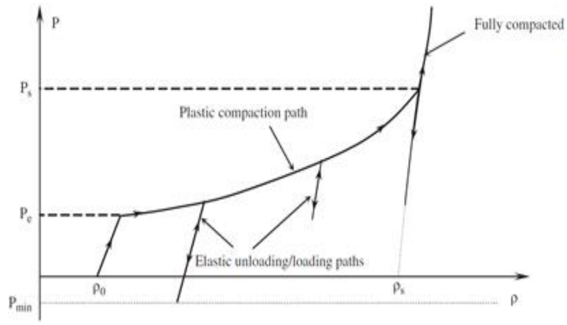

(b) p-ρ relationship

Fig. 9 Concrete equation of state (Herrmann 1969)

$$p = A_1\mu + A_2\mu^2 + A_3\mu^3 + (B_0 + B_1\mu)\rho_0 e \ , \quad \mu > 0\ (compression)$$
$$p = T_1\mu + T_2\mu^2 + B_0\,\rho_0 e\ , \ \ \mu > 0\ (tension) \tag{10}$$

Where p is the pressure; $\mu = {}^{\rho}/_{\rho_0} - 1$ where ρ is the density of concrete at any instant, and ρ_0 is full compaction density of concrete at zero pressure; e is the internal energy per unit mass and $A_1, A_2, A_3, B_0, B_1, T_1, T_2$ are material constants.

For the concrete strength model and failure model, RHT model was nominated for modelling concrete as mentioned above. Table 5 shows the properties of the concrete material used in this numerical study after modifying the effective RHT parameters according to the numerical results obtained from the compression and tension tests, as shown in section 3.

5. Mesh sensitivity

One of the main factors which affect the accuracy of numerical results is selecting a proper element size. A serious of convergence numerical simulation were applied to evaluate the mesh sensitivity and ensure the numerical model accuracy. For the 2D explosion wedge modelling, it was found that choosing element size of 1 mm for simulating 4 Kg TNT gives maximum peak overpressures agree well with that calculated from CONWEP with an acceptable error of 6.6%. After mapping the blast wedge from 2D to 3D, an air block was created with consistent

Table 5 Material data of concrete used in this study (ANSYS-AUTODYN 2009)

Equation of state	*P* alpha
Reference Density (g/cm^3)	2.75
Porous density (g/cm^3)	2.314
Porous soundspeed (m/s)	2.92 e+03
Initial compaction pressure (kPa)	2.33 e+04
Solid compaction pressure (kPa)	6.00 e+6
Compaction exponent	3
Solid EOS	Polynomial
Bulk modulus A1 (kPa)	3.527 e+7
Parameter *A*2 (kPa)	3.958 e+7
Parameter *A*3 (kPa)	9.04 e+6
Parameter *B*0	1.22
Parameter *B*1	1.22
Parameter *T*1 (kPa)	3.527 e+7
Parameter *T*2 (kPa)	0
Reference temperature (k)	300
Specific heat (J/kgK)	654
Thermal conductivity (J/mKs)	0
Compaction curve	Standard
Strength	RHT concrete
Shear modulus *G* (kPa)	1.67 e+07
Compressive strength f_c (kPa)	3.5 e+04
Tensile strength (f_t/f_c)	0.1
Shear Strength (f_s/f_c)	0.18
Intact failure surface constant *A*	1.6
Intact failure surface exponent *N*	0.61
Tens. /Comp. meridian ratio (*Q*)	0.6805
Brittle to ductile transition	0.0105
G (elastic)/(elastic-plastic)	2
Elastic strength f_t	0.7
Elastic strength f_c	0.53
Fractured Strength Constant *B*	0.9
Fractured Strength Exponent *M*	0.9
Compressive strain-rate exponent α	0.032
Tensile strain-rate exponent δ	0.036
Max. fracture strength ratio	1.00 e+20
Use CAP on elastic surface?	Yes
Failure	RHT concrete
Damage Constant D_1	0.02
Damage Constant D_2	1
Minimum Strain to Failure e_{min}^{fail}	0.002
Residual Shear Modulus Fraction	0.13
Tensile Failure	Hydro (Pmin)
Erosion	Geometric strain
Erosion strain	2
Type of geometric strain	Instantaneous

dimensions to cover the entire PC slab and the blast fireball. For the 3D modelling, different element sizes of 1, 2, 4, 6, 10, 15 and 20 mm were used. It was found that the smaller the mesh size the more accurate the result. It was noted that when the mesh size is less than 10 mm, the program creates a memory allocation error (ANSYS-AUTODYN 2009). For mesh sizes 10, 15 and 20 mm, the errors are 3.9%, 6.1% and 11.1%, respectively. Accordingly, an element size of 10 mm was used for modelling the air block. In this study, a total of more than 2.3 million elements was used to model

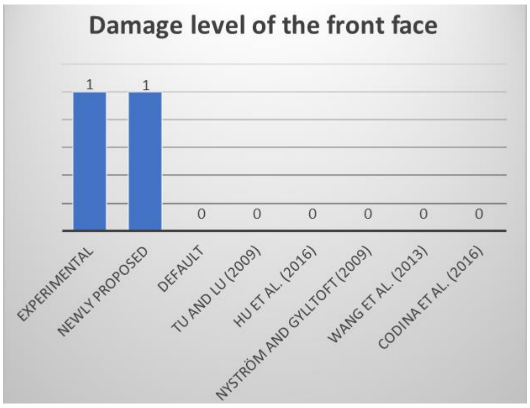

(a) Front face

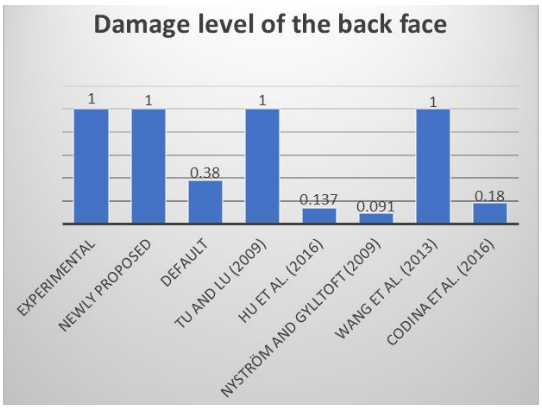

(b) Back face

Fig. 10 Damage levels of the midpoint of the front and back faces of the PC slab of the experimental test and that observed from the numerical simulation using the default, newly proposed and previously proposed RHT model

the air block.

For the concrete slab, a mesh size of 10 mm was adopted to be consistent with the selected element size for the air block and the TNT. In numerical modeling, the element size of the donor boundary environment (i.e., the air block and the TNT) should be equal or smaller than that of the acceptor body (i.e., RC slab) in order to get a more realistic behavior as in the physical tests (ANSYS-AUTODYN 2009). In addition, based on similar numerical models (Wang *et al*. 2013, Luccioni *et al*. 2013, Li *et al*. 2016), it was found that a mesh of 10 mm gives enough accuracy. In this study, a total of 54,621 elements was used to model the PC slab.

6. Comparison of the experimental and numerical results

Fig. 10 shows the damage levels (DL) of the PC slab at the midpoint of the front and back faces observed during the field test and numerical simulations. The DL can be categorized into four levels according to References (Xu and Lu 2006, Zhou and Hao 2008, Wang and Zhang 2014): (1) no damage (DL=0 to 0.1), where the RC slab is still in the intact state with small damage area (spots) on the surface; (2) slight damage (DL=0.1 to 0.3), where the slabs

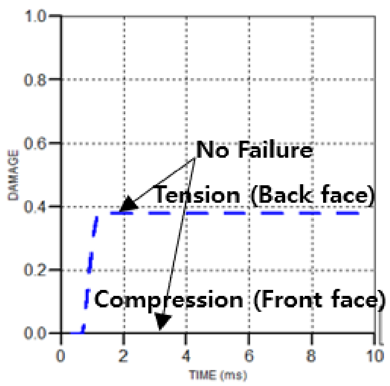

(a) Using default RHT parameters

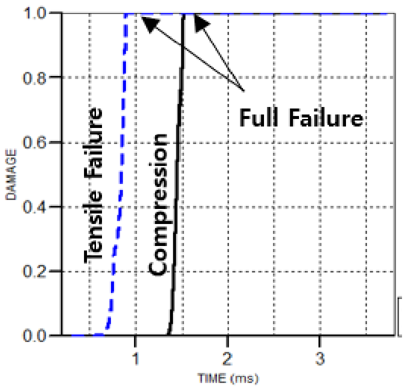

(b) Using proposed RHT parameters

Fig. 11 Damage level time history of the midpoint of the front and back face of PC slab using the default RHT parameters and the proposed RHT parameters

experienced small (hair) cracks; (3) medium damage (DL=0.4 to 0.7), where the slab suffers significant cracks but still in the coherent state; (4) severe damage (DL=0.8 to 1.0), where the slab is totally damaged and fragmented. After doing the field blast test, the center of both the front and back faces are completely damaged. Hence, the DL shall be 1 for both the front and back faces. When comparing this physical damage level with the numerical results using the default RHT parameters, it was noticed that the DL simulated for the front and back faces of the PC slab were 0 and 0.38, respectively. This shows that the default RHT model cannot accurately model the DL of the midpoint of the front and back faces of the simply supported PC slab. In the case of using the previous modified RHT models, only the modified RHT models proposed by Tu and Lu (2007, 2010) and Wang *et al.* (2013) can accurately simulate the DL at the midpoint of the back face of the PC slab. In addition, none of them can simulate the physical DL for the front face well. On the other hand, the newly proposed RHT model accurately simulates the DL at the midpoints of front and back faces of the PC slab well. This shows that the newly proposed RHT model can be used effectively to simulate the DL for the simply supported PC slab under free air blast load. For the PC slab with the proposed parameters, both the front and the back sides experienced a full compression and tensile failure respectively. Also, the tensile failure occurred before the compression failure, as shown in Fig. 11(b). Accordingly, these results indicate that the proposed RHT model simulates a more realistic behaviour of the PC slab than the default RHT model based on with the experimental results.

In addition to the DL study, the crack trajectory and the overall damage pattern recorded from the experimental test were compared to the numerical simulation using the newly proposed RHT model and compared with the other previously modified RHT models (Tu and Lu 2009, Tu and Lu 2010, Hu *et al.* 2016, Nyström and Gylltoft 2009, Nyström and Gylltoft 2011, Wang *et al.* 2013, Codina *et al.* 2016). Table 6 shows the default and the different RHT parameters used in this numerical study. Fig. 12 shows the

Table 6 shows the default, the previous and the newly proposed RHT parameters

Parameters	Default RHT model	Tu and Lu (2007, 2010)	Hu *et al.* (2016)	Nyström and Gylltoft (2009)	Wang *et al.* (2013)	Codina *et al.* (2016)	Proposed RHT model
Reference Density (g/cm^3)	2.75	2.75	2.75	2.75	2.55	2.55	2.75
Compressive strength, f_c (kPa)	3.5 e+04	3.95 e+04	4.0 e+04	3.5 e+04	3.95 e+04	3.0 e+04	3.5 e+04
Shear modulus, G (kPa)	1.67 e+07	2.8 e+07	1.67 e+07	1.67 e+07	2.8 e+07	1.67 e+07	1.67 e+07
Fractured Strength constant, B	1.6	0.7	1.1	1.6	0.7	0.35	0.9
Fractured Strength Exponent, M	0.61	0.8	0.9	0.61	0.8	0.55	0.9
Damage Constant, D_1	0.04	0.015	0.02	0.04	0.015	0.08	0.02
Minimum Strain to Failure e_{min}^{fail}	0.01	8 e-04	0.001	0.01	8 e-04	0.03	0.002
Tensile Failure	Hydro (Pmin)	Hydro (Pmin)	Principal stress	Principal stress	Hydro (Pmin)	Hydro (Pmin)	Hydro (Pmin)
Tensile Failure Stress (kPa)	--------	--------	4.00e+03	3.50e+03	--------	--------	--------
Fracture Energy (j/m^2)	--------	--------	80	120	--------	--------	--------
Crack Softening	--------	--------	yes	yes	--------	--------	--------

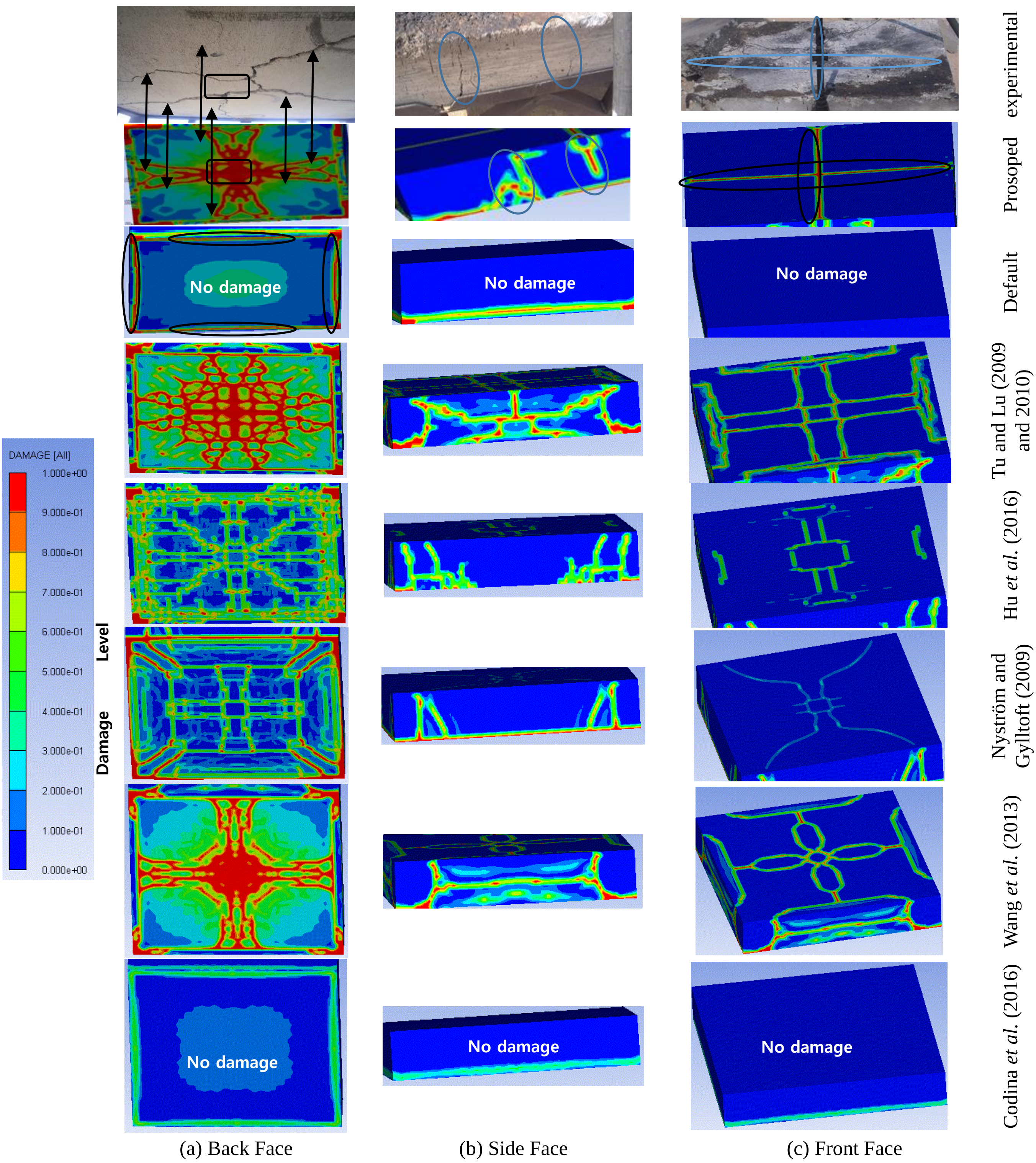

Fig. 12 Experimental and numerical damage pattern observations on the PC slab

overall damage pattern observed between the experimental and the numerical simulations. The damage level scale is shown on the left of the figure. The results show that the newly proposed RHT model can simulate the hyperdynamic behaviour of simply supported PC slab under free blast loads more accurate than the previously modified RHT models. The RHT model proposed by Tu and Lu (2009, 2010) overestimates the damage pattern and crack trajectory on the front face, back faces and the side of the PC slab. The RHT model proposed by Hu *et al.* (2016) underestimates the damage pattern on the front and back faces and no cracks observed on the sides. The RHT model proposed by Nyström and Gylltoft (2009) gives very different crack patterns in the front and back faces. Similarly, the RHT model proposed by Wang *et al.* (2013) overestimates the damage pattern and crack trajectory on the back face of the PC slab and the crack pattern on the front face is different to that observed in the experimental test. The RHT model proposed by Codina *et al*. (2016) appears to be too strong, where it does not predict any damage in either front or back faces.

7. Conclusions

Concrete structure is one of the most used structural material for blast resistant design. Due to the heterogeneity nature of the concrete, it is difficult to simulate the hyperdynamic behaviour and crack trajectory of the concrete material. In the past, multiple RHT models have been proposed. These models have been well calibrated to various concrete structures subjected to different loading and boundary conditions. In this paper, a new set of RHT parameter was proposed to simulate the simply supported PC slab under free blast load. The result shows that the newly proposed RHT model can improves the softening behaviour of the stress-strain curves under the three different loading patterns for compression and tension cases and accurately simulate the failure mode and crack trajectory based on the experimental results. As for the previously defined RHT models, the result shows that the aforementioned proposed RHT models cannot accurately model the nonlinear behaviour of simply supported PC slab under free blast load. In contrast, the newly proposed set of RHT parameters can be used to accurately simulate the damage pattern and the crack trajectory of simply supported PC slab subjected to free air blast loads.

Conflict of Interests

The authors declare that there is no conflict of interests regarding the publication of this paper.

Acknowledgments

The authors are grateful to the financial support by the Egyptian army, International Joint Research Laboratory of Earthquake Engineering (ILEE), National Science Foundation China (grant number: 51778486), Mitacs Globalink Research Award, the State Key Laboratory of Disaster Reduction in Civil Engineering in Tongji University and the State Key Laboratory of Disaster Prevention & Mitigation of the College of Defence Engineering of the Army Engineering University of PLA. Also, the authors are thankful to the manufactural assistance and the technical information provided by Military Technical College, Spring and Transport Needs Manufacturing Company, and Technical Research Centre in Egypt.

References

ANSYS-AUTODYN (2009), "Interactive non-linear dynamic analysis software", Version 16, User's Manual, Century Dynamics Inc.

ANSYS (2007), Theory Reference Manual, Release 11.0, ANSYS Inc.

Benson, D.J. (1992), "Computational methods in Lagrangian and Eulerian hydrocode", *Comput. Meth. Appl. Mech. Eng*., **99**, 2356-2394.

Chen, W.F. (1982), *Plasticity in Reinforced Concrete*, McGraw-Hill, New York, NY, USA.

Codina, R., Ambrosini, D. and de Borbón, F. (2016), "Experimental and numerical study of a RC member under a close-in blast loading", *Eng. Struct*., **127**, 145-158.

CONWEP (1990), Conventional Weapons Effects, Computer Software Produced by the U.S. Army Waterways, Experimental Station, Mississippi, USA.

Gebbeken, N. and Ruppert, M. (2000), "A new material model for concrete in high-dynamic hydrocode simulations", *Arch. Appl. Mech*., **70**, 463-478.

Govindjee, S., Gregory, J.K. and Simo, J.C. (1995), "Anisotropic modeling and numerical-simulation of brittle damage in concrete", *Int. J. Numer. Meth. Eng*., **38**, 3611-3633.

Hentz, S., Donzé, F.V. and Daudeville, L. (2004), "Discrete element modelling of concrete submitted to dynamic loading at high strain rates", *Comput. Struct*., **82**, 2509-2524.

Herrmann, W. (1969), "Constitutive equation for the dynamic compaction of ductile porous materials", *J. Appl. Phys*., **40**, 2490-2499.

Hu, G., Wu, J. and Li, L. (2016), "Advanced concrete model in hydrocode to simulate concrete structures under blast loading", *Adv. Civil Eng*., **2016**, 1-13.

Li, X., Miao, C., Wang, Q. and Geng, Z. (2016), "Antiknock performance of interlayered high-damping-rubber blast door under thermobaric shock wave", *Shock Vib*., **2016**, Article ID 2420893, 9.

Lu, X. and Hsu, C.T.T. (2007), "Stress-strain relations of high-strength concrete under triaxial compression", *J. Mater. Civil Eng*., **19**(3), 261-8.

Luccioni, B., Araoz, G. and Labanda, N. (2013), "Defining Erosion Limit for Concrete", *Int. J. Protect. Struct*., **4**(3), 315-340.

Malvar, L.J., Crawford, J.E., Wesevich, J.W. and Simons, D. (1997), "A plasticity concrete material model for DYNA3D", *Int. J. Impact Eng*., **19**, 847-873.

Nyström, U. and Gylltoft, K. (2009), "Numerical studies of the combined effects of blast and fragment loading", *Int. J. Impact Eng*., **36**(8), 995-1005.

Nyström, U. and Gylltoft, K. (2011), "Comparative numerical studies of projectile impacts on plain and steel-fibre reinforced concrete", *Int. J. Impact Eng*., **38**(2), 95-105.

Rashad, M. and Yang, T.Y. (2018), "Numerical study of steel sandwich plates with RPF and VR cores materials under free air blast loads", *Steel Compos. Struct*., **27**(6), 717-725.

Rashad, M., Wahab, M.M.A. and Yang, T.Y. (2019), "Experimental and numerical investigation of RC sandwich panels with helical springs under free air blast loads", *Steel Compos. Struct*., **30**(3), 217-230.

Riedel, W. (2000), "Beton unter dynamischen Lasten Meso- und makromechanische Modelle und ihre Parameter", Doctoral Thesis, Institut Kurzzeitdynamik, Ernst-Mach-Institut der Bundeswehr Munchen, Freiburg. (in German)

Riedel, W. (2009), "10 years RHT: A review of concrete modelling and hydrocode applications", *Predictive Modeling of Dynamic Processes*, Springer, Boston.

Riedel, W., Thoma, K. and Hiermaier, S. (1999), "Penetration of reinforced concrete by BETA-B-500 numerical analysis using a new macroscopic concrete model for hydrocodes", *Proceedings of the 9th International Symposium Interact*, Eff. Munitions with Struct., Berlin-Strausberg, May.

Riedel, W., Wicklein, M. and Thoma, K. (2008), "Shock properties

of conventional and high strength concrete: Experimental and mesomechanical analysis”, *Int. J. Impact Eng*., **35**, 155-171.
TM5-1300 (1990), Structures to Resist the Effects of Accidental Explosions, Technical Manual, US Department of the Army, Washington DC, USA.
Tu, Z. and Lu, Y. (2009), “Evaluation of typical concrete material models used in hydrocodes for high dynamic response simulations”, *Int. J. Impact Eng*., **36**(1), 132-146.
Tu, Z. and Lu, Y. (2010), “Modifications of RHT material model for improved numerical simulation of dynamic response of concrete”, *Int. J. Impact Eng*., **37**(10), 1072-1082.
Wang, G. and Zhang, S. (2014), “Damage prediction of concrete gravity dams subjected to underwater explosion shock loading”, *Eng. Fail. Anal*., **39**, 72-91.
Wang, W., Zhang, D., Lu, F., Wang, S.C. and Tang, F. (2013), “Experimental study and numerical simulation of the damage mode of a square reinforced concrete slab under close-in explosion”, *Eng. Fail. Anal*., **27**, 41-51.
Xu, K. and Lu, Y. (2006), “Numerical simulation study of spallation in reinforced concrete plates subjected to blast loading”, *Comput. Struct*., **84**(5-6), 431-438.
Zhang, M.H., Sharif, S.H. and Lu, G. (2007), “Impact resistance of high-strength fibre-reinforced concrete”, *Mag. Concrete Res.*, **59**(3), 199-210.
Zhou, X.Q. and Hao, H. (2008), “Numerical prediction of reinforced concrete exterior wall response to blast loading”, *Adv. Struct. Eng*., **11**(4), 355-367.

CC